Research Paper

High-mobility group box-1 impedes skeletal muscle regeneration via downregulation of Pax-7 synthesis by increasing miR-342-5p expression

Trung-Loc Ho[1,*], Yu-Liang Lai[2,3,4,*], Chin-Jung Hsu[5,6], Chen-Ming Su[7], Chih-Hsin Tang[1,8,9,10,11]

[1]Graduate Institute of Biomedical Sciences, College of Medicine, China Medical University, Taichung, Taiwan
[2]Department of Physical Medicine and Rehabilitation, China Medical University Hsinchu Hospital, Hsinchu, Taiwan
[3]Department of Physical Therapy and Graduate Institute of Rehabilitation Science, China Medical University, Taichung, Taiwan
[4]Department of Physical Medicine and Rehabilitation, China Medical University Hospital, Taichung, Taiwan
[5]School of Chinese Medicine, China Medical University, Taichung, Taiwan
[6]Department of Orthopedic Surgery, China Medical University Hospital, Taichung, Taiwan
[7]Department of Sports Medicine, China Medical University, Taichung, Taiwan
[8]Department of Pharmacology, School of Medicine, China Medical University, Taichung, Taiwan
[9]Chinese Medicine Research Center, China Medical University, Taichung, Taiwan
[10]Department of Medical Laboratory Science and Biotechnology, College of Health Science, Asia University, Taichung, Taiwan
[11]Department of Medical Research, China Medical University Hsinchu Hospital, Hsinchu, Taiwan
[*]Equal contribution

Correspondence to: Chen-Ming Su, Chih-Hsin Tang; **email:** cmsu@mail.cmu.edu.tw, chtang@mail.cmu.edu.tw
Keywords: muscle regeneration, HMGB1, Pax-7, myoblasts, miR-342-5p
Received: June 26, 2023 **Accepted:** October 15, 2023 **Published:** November 13, 2023

ABSTRACT

High mobility group box-1 (HMGB1) is a driver of inflammation in various muscular diseases. In a previous study, we determined that HMGB1 induced the atrophy of skeletal muscle by impairing myogenesis. Skeletal muscle regeneration after injury is dependent on pair box 7 (Pax-7)-mediated myogenic differentiation. In the current study, we determined that the HMGB1-induced downregulation of Pax-7 expression in myoblasts inhibited the regeneration of skeletal muscle. We also determined that HMGB1 inhibits Pax-7 and muscle differentiation by increasing miR-342-5p synthesis via receptors for advanced glycation end-products (RAGE), toll-like receptor (TLR) 2, TLR4, and c-Src signaling pathways. In a mouse model involving glycerol-induced muscle injury, the therapeutic inhibition of HMGB1 was shown to rescue Pax-7 expression and muscle regeneration. The HMGB1/Pax-7 axis is a promising therapeutic target to promote muscular regeneration.

INTRODUCTION

Muscle regeneration is a complex process involving the formation of new muscle fibers after injury [1–3]. Muscle regeneration relies on myogenesis, which involves the activation, proliferation, and differentiation of satellite cells or myoblasts [4]. The fusing of myoblasts into multinucleated myotubes results in the enlargement of myofibers, as indicated by the expression of differentiation markers, such as myosin heavy chain (MyHC) [5], desmin [6], or myogenin (MyoG) [7]. Activating myoblast proliferation and regeneration requires various myogenic markers, including myogenic regulatory factors such as pair box 7 (Pax-7), myogenic regulatory

factor 4 (Mrf4), and myogenic factor 5 (Myf5) [8, 9]. Pax-7 has been shown to regulate the conversion of muscle stem cells into myoblasts and participate in other processes related to myogenesis [10]. Pax-7 activation plays a key role in the formation of new muscle fibers after injury [11]. These findings indicate that Pax-7 dysfunction could inhibit the differentiation of skeletal muscle and contribute to impairing muscle regeneration.

MicroRNAs (miRNAs) are a class of small non-coding RNAs that play an essential role in regulating skeletal muscle homeostasis and responding to muscle injury [12, 13]. Myoblast proliferation and differentiation depend on a variety of miRNAs, including miR-22 [14], miR-19 [15], miR-29c [16], and miR-324-5p [13]. However, the role of miRNAs in regulating Pax-7-induced muscle regeneration remains unclear.

High mobility group box-1 (HMGB1) is a ubiquitous nuclear protein that potentiates cellular inflammation [17]. Compared to normal individuals, HMGB1 levels in skeletal muscle are markedly higher in the serum of patients with muscular dystrophy [18] or inflammatory myopathy [19]. Researchers have detected the up-regulation of the HMGB1 gene in a mouse model involving denervation-induced muscle atrophy [20]. Researchers have also demonstrated that in patients with myositis, the interaction of HMGB1 with receptors for advanced glycation end-products (RAGE) or toll-like receptor (TLR) 2 and TLR4 induced the wasting of muscle tissue [21–24]. In a previous study, we demonstrated that HMGB1 treatment impeded myogenesis in myoblast cells. We also observed elevated HMGB1 protein expression in a mouse model involving glycerol-induced muscle injury (GIMI). The oxidation of HMGB1 has been implicated in the development of the dystrophic phenotype, resulting in inflammation and muscle degeneration [18]. HMGB1 can be used as an indicator of muscle atrophy; however, researchers have yet to determine whether the inhibited regeneration of skeletal muscle is due to the HMGB1-induced down-regulation of Pax-7 expression in myoblasts.

RESULTS

HMGB1 inhibits Pax-7 expression and muscle differentiation

Considering the importance of Pax-7 as a marker in muscle regeneration, our objective in the current study was to determine whether HMGB1 affects Pax-7 expression in myoblasts. This was achieved by treating myoblasts with various concentrations of mouse recombinant HMGB1 protein over a period of 24 h. qRT-PCR analysis and western blot assays revealed that HMGB1 significantly inhibited Pax-7 mRNA expression and protein expression, respectively (Figure 1A, 1B). We also explored the effects of HMGB1 on myoblast differentiation through the use of differentiation medium (DM) to initiate the development to myotubes. After three days of DM induction, it was observed that HMGB1 suppressed Pax-7 mRNA and Pax-7 protein expression (Figure 1C, 1D). We also examined the role of Pax-7 in HMGB1-induced muscle regeneration using immunofluorescence double-staining to detect the expression of differentiation markers (Pax-7 and desmin) in GM and DM (Figure 1E). Our results revealed that HMGB1 inhibited differentiation (Pax-7 and desmin expression) in GM and DM (Figure 1F), thereby indicating that HMGB1 suppressed the synthesis of Pax-7, which in turn impaired muscle differentiation activity.

RAGE, TLR2, and TLR4 are involved in HMGB1-inhibited Pax-7 expression and muscle differentiation

Previous studies have shown that RAGE, TLR2, and TLR4 are associated with HMGB1-induced cellular activation [25, 26]. In this study, we sought to identify the receptors that play an important role in the HMGB1-induced inhibition of Pax-7 expression and muscle differentiation. The use of small interfering RNA (siRNA) to knockdown the expression of RAGE, TLR2, and TLR4 receptors was shown to reverse the HMGB1-induced inhibition of Pax-7 mRNA expression (Figure 2A) and protein expression (Figure 2B). Immunofluorescence assays provided further evidence indicating the involvement of RAGE, TLR2, and TLR4 in the HMGB1-induced decrease of muscle differentiation (Figure 2C, 2D). Our results demonstrate that RAGE as well as TLR2 and TLR4 receptors are involved in HMGB1 impairing Pax-7 expression and muscle differentiation.

c-Src signaling is involved in HMGB1-mediated Pax-7 expression and muscle differentiation

One previous study reported that the suppression of cellular Src kinase (c-Src) activity is involved in regulating muscle differentiation [27]. Our objective in the current study was to determine whether c-Src is involved in the HMGB1-induced inhibition of Pax-7 synthesis and skeletal muscle differentiation. We found that incubating myoblasts with 10 ng/mL of HMGB1 significantly enhanced the phosphorylation of c-Src (Figure 3A), the effects of which were abolished by RAGE, TLR2, or TLR4 siRNA (Figure 3B). Pre-treating cells with a c-Src siRNA or c-Src inhibitor (PP2) was shown to restrict the HMGB1-induced decrease in Pax-7 expression (Figure 3C, 3D). Inhibiting c-Src signaling was also shown to reverse the effects of

HMGB1 on muscle differentiation (Figure 3E, 3F). These findings suggest that the effects of HMGB1 on Pax-7 expression and muscle differentiation involve the activation of c-Src signaling via the RAGE, TLR2, and TLR4 receptors.

HMGB1 suppresses Pax-7 synthesis and muscle differentiation by promoting miR-342-5p expression

Research in the field of bioinformatics has revealed that over 30% of the proteins in mammals are regulated by miRNAs [28]. In the current study, we employed publicly available bioinformatics software (TargetScan, miRWalk, and miRDB) to identify the miRNAs that are involved in Pax-7 expression. Cross-checking the three programs revealed 12 miRNAs that bind directly to Pax-7 (Figure 4A). A correlation heat map revealed that miR-185-3p, miR-342-5p, and miR-499-3p were highly expressed in HMGB1-treated myoblasts, leading to their selection for further study (Figure 4B). Our analysis revealed that HMGB1 enhanced the expression of miR-342-5p in a dose-dependent manner (Figure 4C). The HMGB1-induced promotion of miR-342-5p expression was moderated by the presence of RAGE, TLR2, TLR4, c-Src, indicating that miR-342-5p acted downstream from these molecules (Figure 4D). We also sought to determine whether the HMGB1-induced effects on Pax-7 expression depended on miR-342-5p synthesis.

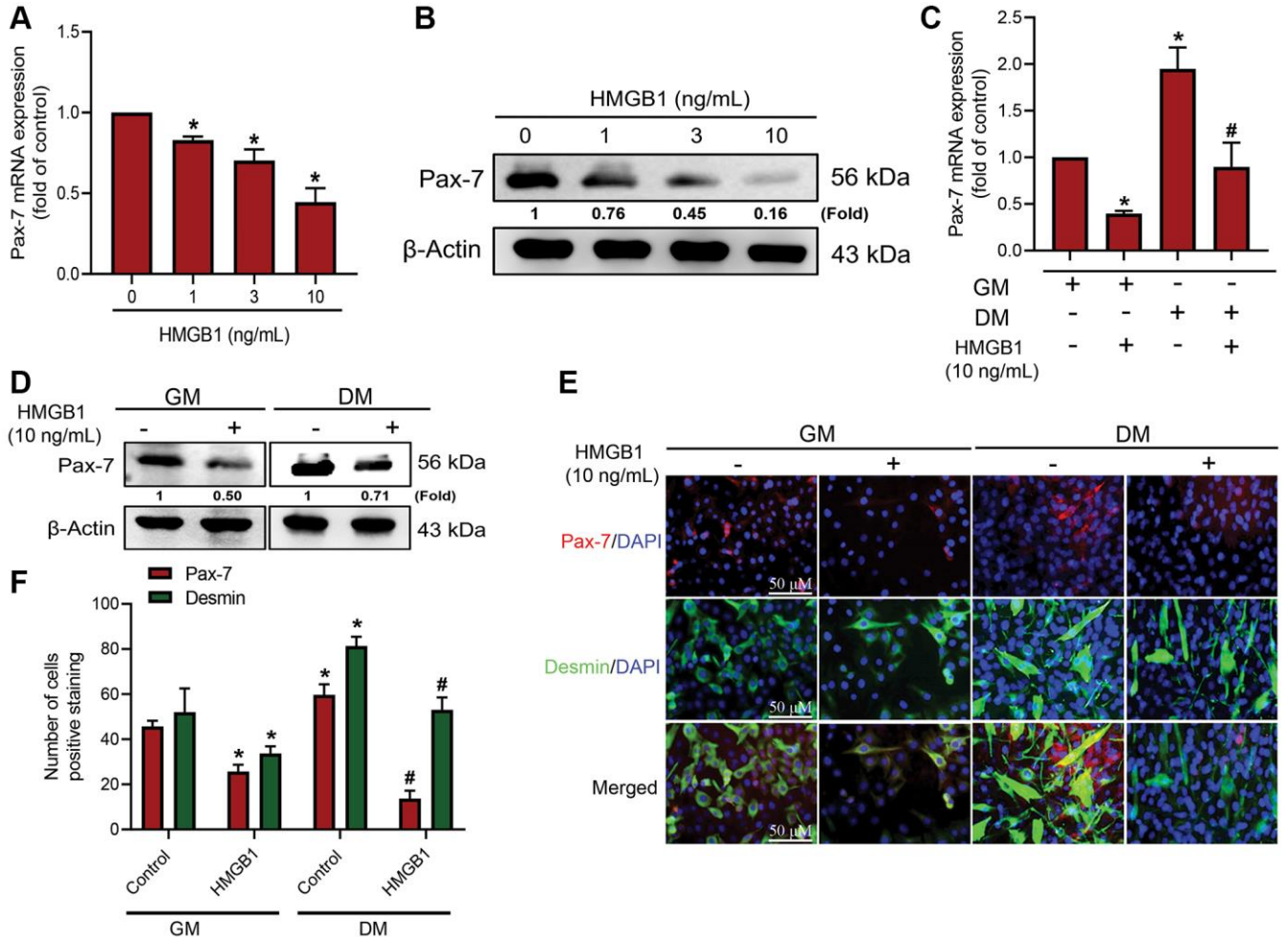

Figure 1. HMGB1 inhibits Pax-7 synthesis in skeletal muscle myoblasts. After exposing C2C12 cells to HMGB1 for 24 h, the expression of Pax-7 mRNA and protein was examined by (**A**) qRT-PCR (n = 3) and (**B**) western blotting assay (n = 3). C2C12 cells were cultured in growth medium (GM) and differentiation medium (DM) for three days with or without HMGB1 (10 ng/mL) for 24 h, after which Pax-7 expression was examined using (**C**) qRT-PCR (n = 3) and (**D**) western blotting assay (n = 3). (**E**) Immunofluorescence staining showing the expression of Pax-7 and desmin in C2C12 cells cultured in GM and DM after HMGB1 treatment (n = 3). Pax-7 is indicated by red coloring, desmin is indicated by green, and DAPI is shown in blue. Scale bars = 50 μm. (**F**) Number of positively stained cells were quantified by ImageJ software (n = 3). β-Actin was used as the loading control. All data are presented as the mean ± SD of triplicate experiments. $^{*}p < 0.05$ compared with control group; $^{\#}p < 0.05$ compared with HMGB1-treated group. Abbreviations: GM: growth medium; DM: differentiation medium.

Transfecting a miR-342-5p inhibitor into myoblasts was shown to reverse the HMGB1-induced reduction in Pax-7 expression and muscle differentiation (Figure 4E–4H). Taken together, it appears that HMGB1 reduces Pax-7 expression and muscle differentiation by promoting the synthesis of miR-342-5p via RAGE, TLR2, TLR4, and c-Src signaling cascades.

Inhibition of HMGB1 reverses GIMI and Pax-7 expression

Intramuscular glycerol injection is a recent approach to inducing muscle injury and subsequent regeneration [29–31]. We previously reported that GIMI can be rescued by inhibiting the effects of HMGB1 using HMGB1 shRNA [32]. H&E staining was used to show the cross-sectional area (CSA) of muscle fibers from the tibialis anterior (TA) (Figure 5A). We then measured the distribution of CSA in the control group, GIMI group, and GIMI+HMGB1 shRNA group. These results indicate that the increase in CSA was more pronounced in the GIMI+HMGB1 shRNA group than in the GIMI group (Figure 5B). HMGB1 shRNA was also shown to restore the protein expression of Pax-7 in skeletal muscle to normal levels (Figure 5C, 5D). The role of Pax-7 in myogenesis was assessed *in vivo* by examining muscle regeneration via immunocytochemical staining. We found that a decrease in Pax-7 protein expression

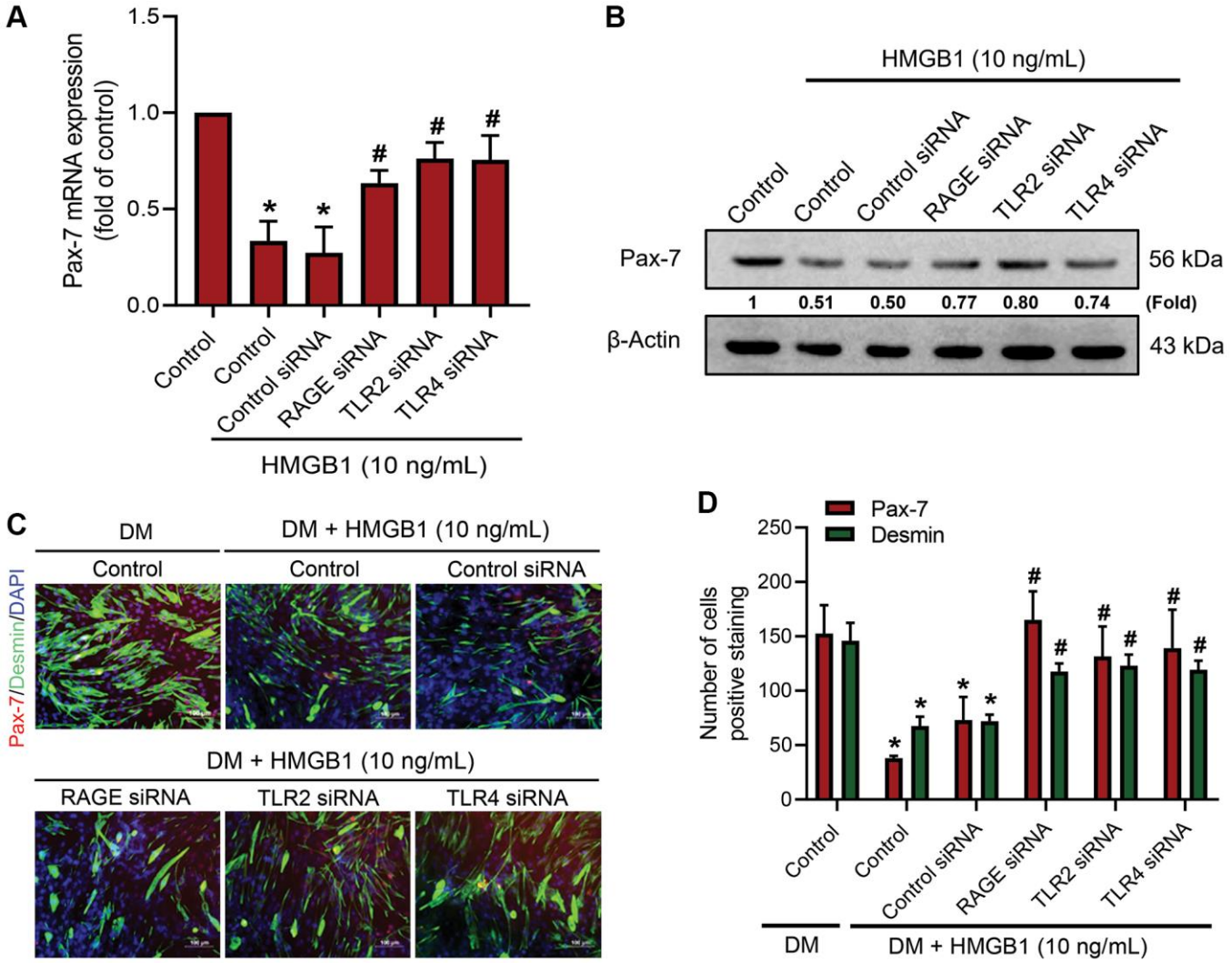

Figure 2. RAGE, TLR2, and TLR4 receptors are involved in the downregulation of Pax-7 expression by HMGB1. C2C12 cells were pre-treated with 100 nM siRNA against RAGE, TLR2, or TLR4 for 24 h and then subjected to HMGB1 (10 ng/mL) stimulation for 24 h. The expression levels of Pax-7 mRNA and protein were respectively analyzed by (**A**) qRT-PCR (n = 3) and (**B**) western blotting assay (n = 3). (**C**) Immunofluorescence staining was used to visualize the expression of Pax-7 and desmin in C2C12 cells in DM after HMGB1 treatment (10 ng/mL) with indicated siRNAs (n = 3). Pax-7 is indicated by red coloring, desmin is indicated by green, and DAPI is shown in blue. Scale bars = 100 μm. (**D**) Number of positively stained cells were quantified by ImageJ software (n = 3). β-Actin was used as the loading control. All data are presented as the mean ± SD of triplicate experiments. $^{*}p < 0.05$ compared with control group; $^{\#}p < 0.05$ compared with HMGB1-treated group.

was correlated with desmin in TA muscle fibers following glycerol injury. Both proteins presented elevated expression levels in the HMGB1 shRNA-treated group (Figure 5E, 5F). In addition, the increasing number of regenerating fiber correlates to the expression of Pax-7 and desmin proteins (Figure 5G). These results indicate that inhibiting HMGB1 ameliorated glycerol-induced muscle damage and subsequent muscle regeneration by restoring Pax-7 expression.

DISCUSSION

It has been established that the regenerative capacity of skeletal muscle involves differentiation and myogenesis [33–36]. Recent research has revealed links between aberrant HMGB1 expression and muscle wasting or dysfunction [19, 37, 38]. In prior investigations, we substantiated that HMGB1, at a concentration of 10 ng/mL, has the capacity to exacerbate skeletal muscle atrophy by impeding various facets of myogenic processes [32]. It has been well-documented that necrotic and immune cells prominently contribute to the active or passive release of HMGB1 into the extracellular milieu [17, 39]. This phenomenon is closely associated with the heightened expression of HMGB1 levels during conditions of muscle loss [40]. Nonetheless, the role of HMGB1 in the regeneration of skeletal muscle has yet to be elucidated. In the current study, we found that HMGB1 inhibits the regeneration of skeletal muscle by downregulating Pax-7 expression and myoblast differentiation capacity. Our qRT-PCR

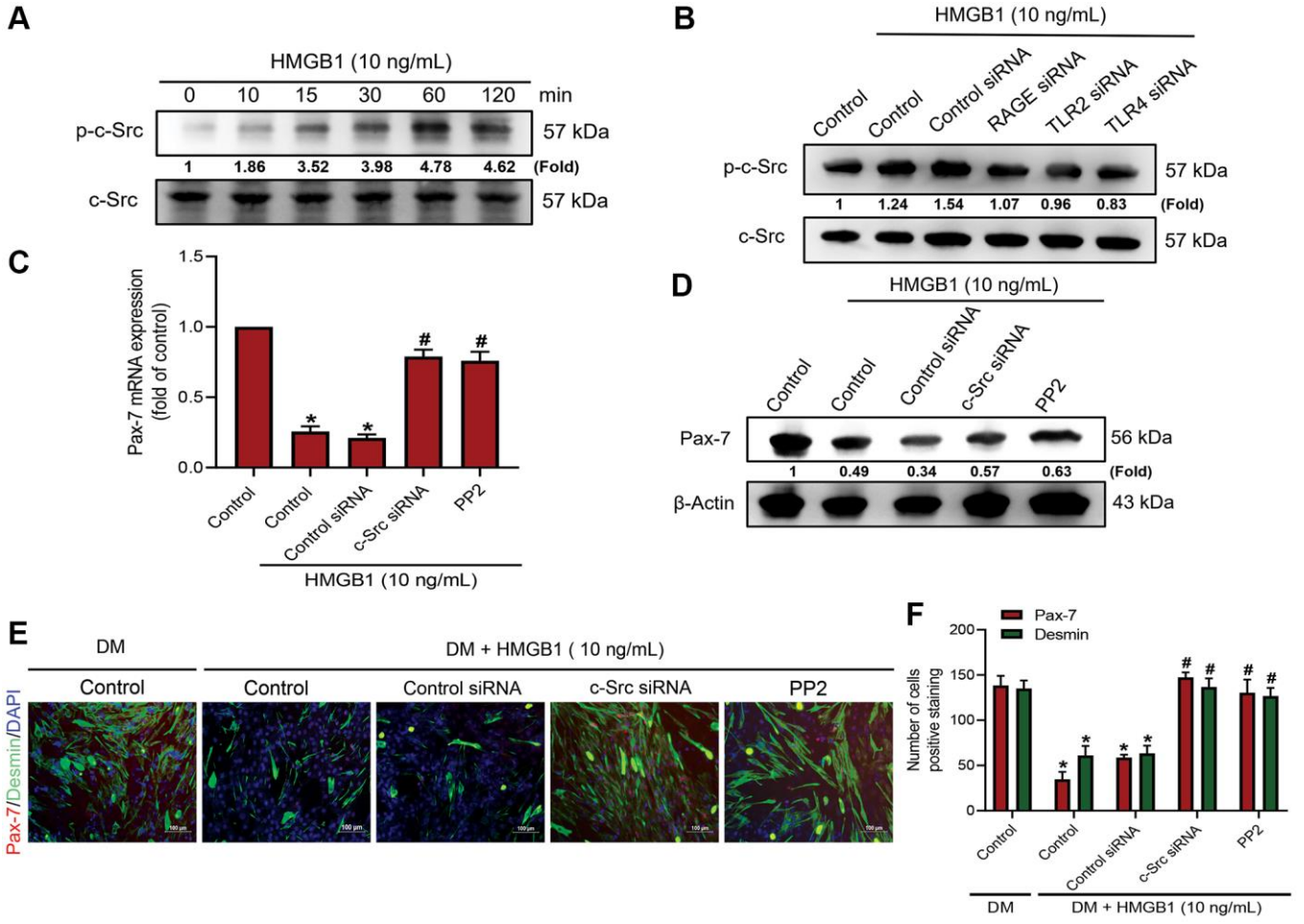

Figure 3. c-Src signaling is involved in HMGB1-mediated Pax-7 expression and muscle differentiation. Western blot analysis of c-Src phosphorylation in (**A**) C2C12 cells treated with HMGB1 (10 ng/mL) following a time-dependent manner (n = 3) and (**B**) C2C12 cells pre-treated with various siRNAs against RAGE, TLR2, and TLR4 molecules (100 nM) and then exposed to HMGB1 (10 ng/mL) for 24 h. (**C**) qRT-PCR (n = 3) and (**D**) western blot analysis of Pax-7 mRNA and protein expression, respectively, in C2C12 cells after HMGB1 co-treatment with c-Src siRNA (100 nM) or c-Src inhibitor (PP2; 1 μM) for 24 h (n = 3). (**E**) Immunofluorescence staining to visualize the expression of Pax-7 and desmin in C2C12 cells in DM after HMGB1 (10 ng/mL) co-treatment with c-Src siRNA (100 nM) or PP2 (1 μM) for 24 h (n = 3). Pax-7 is indicated by red coloring, desmin is indicated by green, and DAPI is shown in blue. Scale bars = 100 μm. (**F**) Number of positively stained cells were quantified by ImageJ software (n = 3). β-Actin was used as the loading control. All data are presented as the mean ± SD of triplicate experiments. $^{*}p < 0.05$ compared with control group; $^{\#}p < 0.05$ compared with HMGB1-treated group.

results revealed that HMGB1 treatment increased miR-342-5p expression in skeletal muscle cells. We also sought to determine whether the link between inhibited Pax-7 expression and decreased muscle differentiation was associated with HMGB1 receptor signaling (RAGE, TLR2, TLR4) or c-Src signaling. This was achieved via treatment with siRNA against RAGE, TLR2, TLR4, c-Src and a c-Src inhibitor. Our results revealed that miR-342-5p acted as a downstream signaling molecule of RAGE, TLR2, TLR4, and c-Src signaling cascades. HMGB1 blockade was shown to promote the regeneration of skeletal muscle in a mouse model involving induced muscular injury. This study provides solid evidence indicating that the inhibition of HMGB1 signaling is a promising therapeutic approach to promoting muscle regeneration. In consistent with our findings, another research group has also shown that the inhibition of HMGB1 oxidative activity expedites the process of regeneration without aggravating inflammation in both muscle and liver tissues, which serve as pivotal paradigms in the fields of regenerative medicine and biology [18, 41]. Interestingly, therapeutic strategies against these specific HMGB1 isoforms can serve as models for more efficient therapeutic strategies against tissue damage [42, 43]. Taken together, the evidence suggests that HMGB1 represents a novel

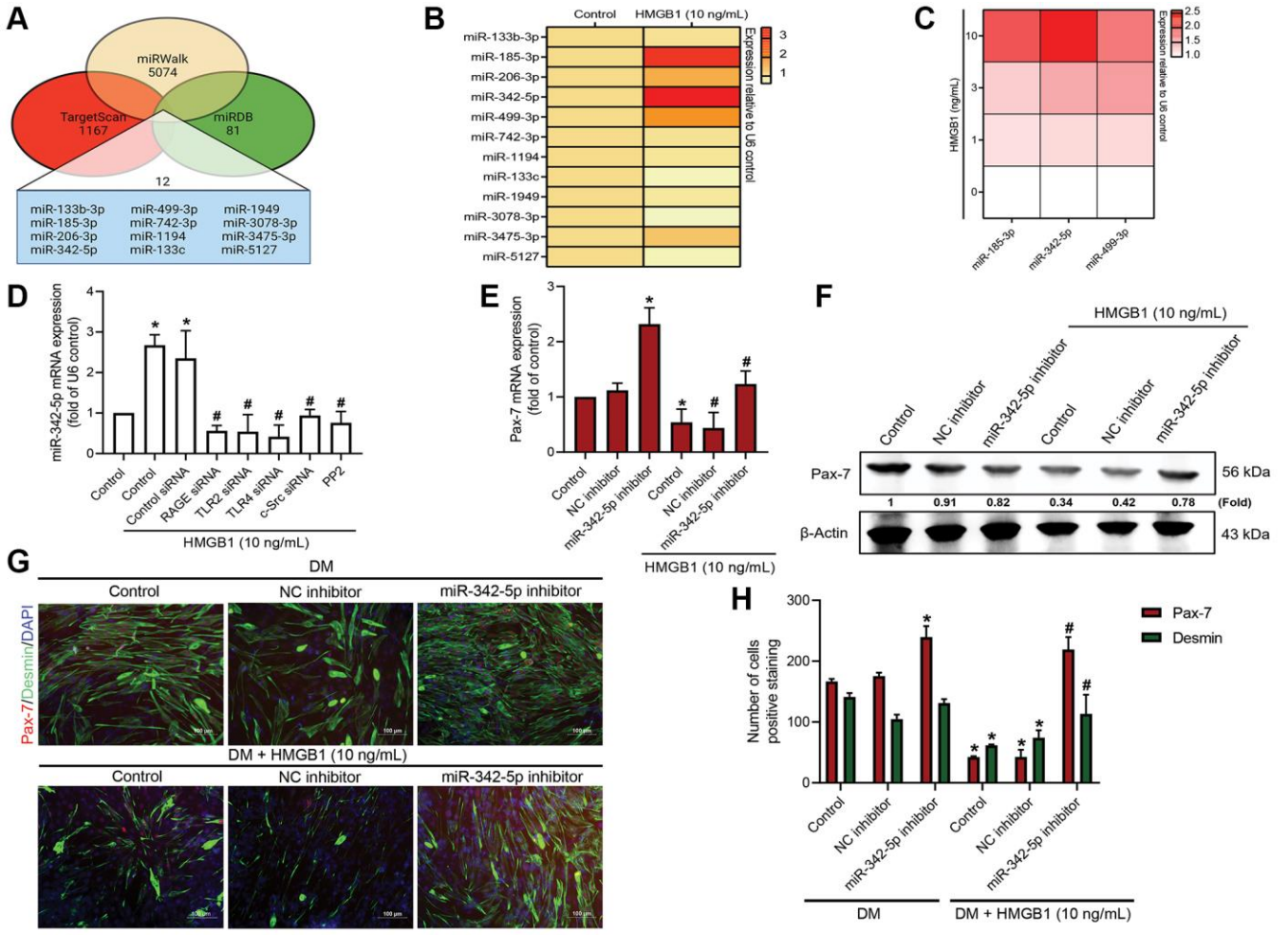

Figure 4. miR-342-5p/Pax-7 axis is involved in HMGB1-induced inhibition of skeletal muscle differentiation. (**A**) Potential miRNA targets of Pax-7 predicted by miRWalk, miRDB, and TargetScan. (**B**) qRT-PCR assays showing the expression of the 12 predicted miRNAs following HMGB1 treatment (10 ng/mL) (n = 3). (**C**) qRT-PCR assays showing the expression of miR-185-3p, miR-342-5p, and miR-499-3p in C2C12 cells after HMGB1 treatment (n = 6). (**D**) qRT-PCR assays showing miR-342-5p expression in C2C12 cells transfected with various siRNAs or pre-treated with c-Src inhibitor (PP2; 1 μM) prior to HMGB1 treatment for 24 h (n = 3). (**E**) qRT-PCR analysis and (**F**) western blot analysis showing the effect of miR-342-5p inhibitor on Pax-7 mRNA expression and protein expression (n = 3), respectively. (**G**) Immunofluorescence staining showing the expression of Pax-7 and desmin in C2C12 cells in DM after HMGB1 treatment (10 ng/mL) with 50 nM of miR-342-5p inhibitor or negative control (n = 3). Pax-7 is indicated by red coloring, desmin is indicated by green, and DAPI is shown in blue. Scale bars = 100 μm. (**H**) Number of positively stained cells were quantified by ImageJ software (n = 3). β-Actin was used as the loading control. All data are presented as the mean ± SD of triplicate experiments. $^{*}p < 0.05$ compared with control group; $^{\#}p < 0.05$ compared with HMGB1-treated group.

signaling molecule deserving of targeted intervention for the enhancement of muscle regeneration.

Previous studies have reported that Pax-7 is a switch molecule capable of inducing the regeneration of skeletal muscle following acute muscle injury [44, 45]. The fact that Pax-7 knockout mice presented a diminished number of muscle satellite cells and impaired muscle regeneration supports the notion that Pax-7 is required for the propagation and function of the satellite cell population [46, 47]. We can therefore surmise that Pax-7 plays an essential role in the activation of skeletal satellite cells; however, the role of Pax-7 expression in myoblast differentiation remains unknown. In the current study, *in vitro* analysis revealed that the expression of Pax-7 markers upregulated the differentiation of skeletal muscle, whereas *in vivo* analysis revealed that Pax-7 expression levels were significantly lower in the muscular atrophy group than in the control group. It was also observed that positive staining for Pax-7 in satellite muscle cells was higher in the HMGB1 shRNA treated-group than in the GIMI group (Figure 5C, 5D). From this, we can deduce that the therapeutic knock-down of HMGB1 signaling ameliorated muscular injury by promoting the expression of Pax-7 regeneration markers.

Notably, a previous histological finding indicated that the degenerative changes resulting from glycerol-induced injury bear a striking resemblance to the

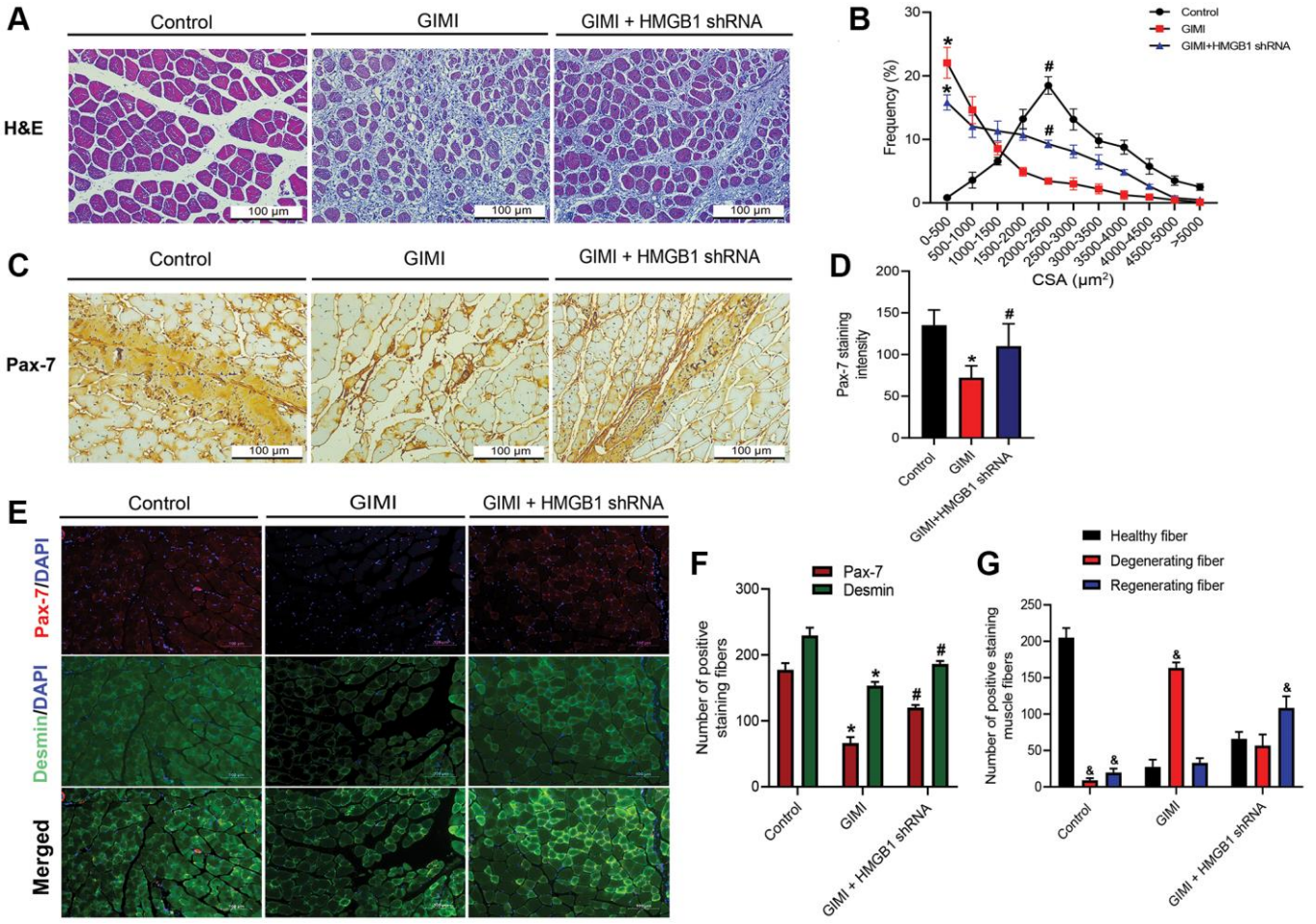

Figure 5. Inhibition of HMGB1 reverses glycerol-induced muscle injury (GIMI) and Pax-7 expression. (**A**) Representative images of H&E-stained tibialis anterior (TA) sections from mice in control group and glycerol-induced muscle injury (GIMI) without or with HMGB1 shRNA treated-group (GIMI+HMGB1 shRNA) (n = 3); scale bars = 100 μm. (**B**) Frequency distribution of cross-sectional area (CSA) of TA muscle fibers (n = 3). (**C**) Immunohistochemistry analysis of Pax-7 protein expression in TA muscle of control group, GIMI group, and GIMI+HMGB1 shRNA group (n = 3). (**D**) Quantification of Pax-7 staining intensity in TA muscle (n = 6). (**E**) Immunofluorescence analysis showing the expression of Pax-7 and desmin in TA muscle in the control, GIMI, and GIMI+HMGB1 shRNA groups (n = 3); scale bars = 100 μm. (**F**) Quantification of the Pax-7 and desmin positive staining fibers in TA muscle were analyzed by ImageJ software (n = 3). (**G**) The healthy fiber (large cells), degenerating fiber (mononuclear in necrotic cells), and regenerating fiber (multinucleated cells) were quantified with the positive double-staining of Pax-7 and desmin by using ImageJ software (n = 3). All data are presented as the mean ± SD of triplicate experiments. $^{\&}p < 0.05$ compared with the healthy fiber; $^{*}p < 0.05$ compared with control group; $^{\#}p < 0.05$ compared with GIMI group.

pathological features observed in Duchenne muscular dystrophy [48]. The intramuscular administration of glycerol has been empirically shown to induce myofiber injury characterized by a degenerative phenotype, as evidenced in rats within a three-day post-injury period [49]. These compelling observations suggest the potential utility of glycerol as a chemical agent for inducing muscle injuries in murine models. Therefore, we used the utilization of intramuscular injection of glycerol as an innovative experimental model for inducing acute muscle injury and triggering skeletal muscle inflammation. The TA muscle has attracted substantial interest as a prominent choice in skeletal muscle injury models, owing to its easily accessible anatomical location and its capacity to consistently produce uniform injury outcomes within 24 h after glycerol injection [48, 50]. Our results demonstrated that glycerol significantly induced TA muscle injury as well as degeneration phenotype in mouse model (Figure 5A, 5B). These outcomes imply that the TA muscle serves as a favourable locus for the induction of muscle injury.

RAGE, TLR2, and TLR4 are the most important HMGB1 receptors affecting the inflammatory response in many cellular diseases [51, 52]. In muscular diseases, RAGE upregulation has been shown to induce atrophy in skeletal muscle [53]. The pharmacological inhibition of TLR4 has been shown to decrease lipopolysaccharide-induced muscle wasting by suppressing the activation of inflammatory and proteolytic pathways [54]. In a previous mouse model, TLR2 knockout was shown to attenuate cardiotoxin-induced atrophy in skeletal muscle [55]. In the current study, the inhibition of RAGE, TLR2, and TLR4 signaling via HMGB1 treatment restored Pax-7 mRNA and protein expression in myoblasts. Taken together, these results confirmed the participation of RAGE, TLR2, and TLR4 receptor signaling in the HMGB1-induced inhibition of myoblast differentiation and Pax-7 synthesis. These results also suggest that the expression of RAGE, TLR2, or TLR4 negatively regulates the regeneration of skeletal muscle.

It is well-known that miRNAs play an essential role in skeletal muscle development via their participation in myogenesis [56], while aberrant miRNA expression has been observed in muscle diseases, including cardiac and skeletal muscle hypertrophy, heart failure, and muscular

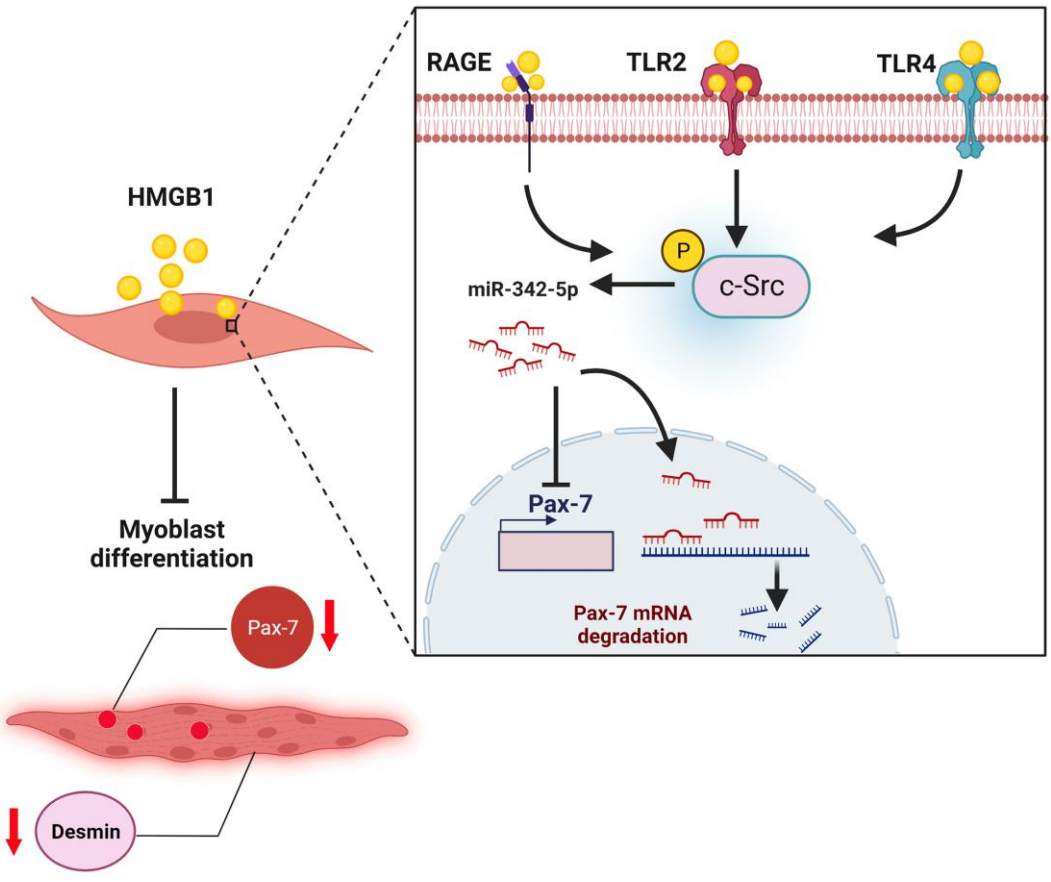

Figure 6. Graphical abstract: schematic illustration of proposed mechanisms underlying the HMGB1-induced inhibition of muscle regeneration, where HMGB1 inhibits Pax-7 expression and skeletal muscle regeneration by promoting the synthesis of miR-342-5p via RAGE, TLR2, TLR4, and c-Src signaling pathways.

dystrophy [57–59]. The expression of muscle-specific miRNAs, such as miR-1 and miR-206, is insufficient to induce differentiation in myoblast cells. Knockdown of endogenous miR-1 and miR-206 in a neonatal mouse model was shown to promote the proliferation of satellite cells and increase Pax-7 protein levels in skeletal muscle [60]. In the current study, the up-regulation of miR-342-5p by HMGB1 suppressing Pax-7 expression and skeletal muscle cell differentiation suggests that miR-342-5p plays an important role in regulating muscle regeneration via Pax-7. Given the substantial dose-dependent elevation of miR-342-5p observed in myoblast cells following treatment with HMGB1 (Figure 4B, 4C), it is reasonable to postulate that miR-342-5p represents a primary target of HMGB1 action. Nonetheless, our examination of the role of miR-342-5p was limited to *in vitro* analysis. Further analysis will be needed to investigate the role of miR-342-5p *in vivo* in animal models involving muscular injury.

In conclusion, this study demonstrated that the HMGB1-induced inhibition of Pax-7 expression impaired skeletal muscle regeneration by promoting the synthesis of miR-342-5p via RAGE, TLR2, TLR4, and c-Src signaling cascades (Figure 6). The therapeutic inhibition of HMGB1 signaling was shown to enhance the regeneration of skeletal muscle by increasing the expression of Pax-7 markers *in vivo*. Our findings suggest that HMGB1 plays key roles in the wasting and regeneration of skeletal muscle.

MATERIALS AND METHODS

Reagents and materials

RAGE (sc-36374), TLR2 (sc-40256), TLR4 (sc-40260), c-Src (sc-29228) siRNAs were obtained from Santa Cruz Biotechnology (Dallas, TX, USA); control siRNA (D-001810-10-05) was purchased from Dharmacon (Lafayette, CO, USA). Recombinant mouse HMGB1 protein was obtained from Biorbyt (orb57027, Cambridge, UK). Pax-7 antibodies were obtained from R&D Systems (NBP2-32894, Minneapolis, MN, USA). Antibodies against c-Src (sc-5266) and p-c-Src (sc-12928-R) were obtained from Santa Cruz Biotechnology (Dallas, TX, USA). Desmin antibodies were obtained from Abcam (ab216616, Eugene, OR, USA). Secondary antibodies goat anti-rabbit Alexa Fluor 488 (#A32731) and rabbit anti-mouse Alexa Flour 594 (#A27027) were obtained from Thermo Fisher Scientific (Waltham, MA, USA). PP2 inhibitors (purity > 98%, #CAS 172889-27-9) and DAPI dye (#CAS D9564) were purchased from Sigma-Aldrich (St. Louis, MO, USA). miR-342-5p inhibitor (#65522) and NC miRNA inhibitor (#135060) were purchased from AllBio Science (Taichung City, Taiwan). Mouse shRNA HMGB1 plasmid (Cat#TRCN0000365913) was purchased from National RNAi Core Facility (Sinica, Taiwan), and puro-HMGB1 shRNA-Pmd CMV constructs were purchased from Addgene (Watertown, MA, USA). All *in vivo* reagents and materials were referred to our previous study [32].

Cell cultures and muscle differentiation

C2C12 myoblasts obtained from the American Type Culture Collection (ATCC, Manassas, VA, USA) [32] were cultured in a growth medium (GM) of Dulbecco's modified Eagle medium (DMEM) supplemented with 10% fetal bovine serum and penicillin (100 U/mL) (Thermo Fisher Scientific, Waltham, MA, USA). The cells were differentiated into myotubes by changing the growth medium to differentiation medium (DM) for 72 h [61, 62], which consisted of DMEM containing 2% horse serum (Thermo Fisher Scientific, Waltham, MA, USA).

Transfection assay

C2C12 cells were transfected with RAGE, TLR2, TLR4, c-Src, and control siRNAs or miR-342-5p inhibitors or negative control (NC) miRNA inhibitors by using Lipofectamine2000™ reagent (Thermo Fisher Scientific, Waltham, MA, USA) for 20 min at room temperature according to the manufacturer's instructions. The mixtures were then applied to the cells in a volume of Opti-MEM™ I (Gibco, Grand Island, NY, USA), giving a final concentration of 100 nM siRNA and 50 nM miRNA-inhibitor for 24 h.

Quantitative Real-time Polymerase Chain Reaction (qRT-PCR) analysis of mRNA and miRNA

Total RNA was extracted from myoblasts using TRIzol™ reagent (MDBio, Taipei, Taiwan) in accordance with the manufacturer's instructions. qRT-PCR analysis was performed using the methods outlined in our previous reports [32, 63]. Briefly, 1 μg of total RNA was reverse transcribed to complementary DNA (cDNA) with the oligo-DT primer. cDNA was synthesized using the MMLV reverse transcriptase system (Invitrogen, Carlsbad, CA, USA). miRNA was synthesized using the Mir-X™ miRNA First-Strand Synthesis kit (Terra Bella Avenue, Mountain View, CA, USA) in accordance with the manufacturer's instructions. qRT-PCR analysis was performed using the Fast SYBR® Green Mix in the StepOnePlusTM system (Applied Biosystems, Foster City, CA, USA). The primers used in this study are listed in Supplementary Table 1. Glyceraldehyde-3-phosphate dehydrogenase (GAPDH) mRNA was used as reference for mRNA quantification, and U6 small nuclear RNA (U6 snRNA) was used for miRNA. The

$2^{-\Delta\Delta CT}$ method was used to quantify the qRT-PCR analyses [64]. The result of this method is presented as the fold change of target gene expression in a target sample which is relative to a reference sample normalized to a reference gene.

Western blot analysis

Total protein (30 μg) from myoblast cell lysate was separated via SDS-PAGE electrophoresis and then transferred to Immobilon® PVDF membranes using the protocols outlined in our previous reports [32, 65, 66]. The membranes were blocked in TBST (TBS with 0.1% Tween 20) with 5% skim milk at room temperature for 1 h and then incubated overnight in primary antibodies at 4°C. The membranes were then incubated in TBST with secondary antibodies at room temperature for 1 h. The proteins were imaged on an Immobilon chemiluminescent HRP substrate using an ImageQuantTM LAS 4000 biomolecular imager (G.E. Healthcare, Little Chalfont, UK).

Immunofluorescence staining

Immunofluorescence staining was performed following the protocol outlined in our previous reports [32]. Briefly, the cells were fixed in 3.7% paraformaldehyde at room temperature for 30 min, permeabilized with 0.1% Triton™ X-100 for 10 min and blocked with 1% bovine serum albumin (BSA) at room temperature for 1 h, prior to labeling with rabbit anti-desmin primary antibodies (1:500) and mouse-anti Pax-7 primary antibodies (1:100) at 4°C overnight. The cells were then washed twice using 1X PBS and incubated with Alexa Fluor 488 goat anti-rabbit (1:1000) and Alexa Flour 594 rabbit anti-mouse (1:1000) secondary antibodies at room temperature for 1 h. Finally, the cells were then washed twice before counterstaining the nuclei with DAPI for 10 min. Images were captured using Nikon ECLIPSE TE300 Inverted Microscope (Nikon Tokyo, Japan). The total number of immunofluorescent positive staining cells in each group was counted and quantified by ImageJ software (n = 3 per group).

Immunohistochemical (IHC) staining

Sections of skeletal muscle tissue were embedded in paraffin and then rehydrated and stained using a hematoxylin and eosin (H&E) kit and IHC Kit (Sigma-Aldrich, St. Louis, MO, USA) in accordance with the manufacturer's instructions.

Bioinformatics screening of direct miRNA targets of Pax-7 expression

Analysis of miRNAs binding to the 3′UTR of Pax-7 was performed using publicly available bioinformatics software (TargetScan: https://www.targetscan.org; miRWalk: mirwalk.umm.uni-heidelberg.de; miRDB: https://mirdb.org/). 12 miRNAs were identified (miR-133b-3p, miR-185-3p, miR-206-3p, miR-342-5p, miR-499-3p, miR-742-3p, miR-1194, miR-133c, miR-1949, miR-3078-3p, miR-3475-3p, and miR-5127) that could bind most effectively with Pax-7.

Statistical analysis

Statistical analysis included unpaired Student's *t*-tests in the comparison of two groups and one-way analysis of variance (ANOVA) tests involving comparisons of more than two groups. Results are presented as the mean ± standard deviation (SD) of at least three independent experiments. Between-group differences were considered significant if the *p*-values were less than 0.05.

AUTHOR CONTRIBUTIONS

C.-H Tang and C.-M Su supervised the research and provided financial support. C.-H Tang, C.-M Su, T.-L Ho and L.-Y Lai designed the study conception. T.-L Ho performed the experiments. J.-C Hsu, C.-M Su, and T.-L Ho analyzed the data and prepared manuscript. All authors approved the final version to be published.

CONFLICTS OF INTEREST

The authors declare no conflicts of interest related to this study.

ETHICAL STATEMENT

The animal study and protocols were approved by the Institutional Animal Care and Use Committee of China Medical University (IACUC Approval No: 2022-205).

FUNDING

This work was supported by grants from the China Medical University Hsinchu Hospital (CMUHCH-DMR-112-016); China Medical University Hospital (DMR-112-088); National Science and Technology Council (NSTC 112-2314-B-039-038-MY3); China Medical University (CMU110-N-23); Taiwan's Ministry of Science and Technology (MOST 111-2320-B-039-022-MY3).

REFERENCES

1. Forcina L, Cosentino M, Musarò A. Mechanisms Regulating Muscle Regeneration: Insights into the Interrelated and Time-Dependent Phases of Tissue Healing. Cells. 2020; 9:1297.

https://doi.org/10.3390/cells9051297
PMID:32456017

2. Yang W, Hu P. Skeletal muscle regeneration is modulated by inflammation. J Orthop Translat. 2018; 13:25–32.
https://doi.org/10.1016/j.jot.2018.01.002
PMID:29662788

3. Chargé SB, Rudnicki MA. Cellular and molecular regulation of muscle regeneration. Physiol Rev. 2004; 84:209–38.
https://doi.org/10.1152/physrev.00019.2003
PMID:14715915

4. Schmidt M, Schüler SC, Hüttner SS, von Eyss B, von Maltzahn J. Adult stem cells at work: regenerating skeletal muscle. Cell Mol Life Sci. 2019; 76:2559–70.
https://doi.org/10.1007/s00018-019-03093-6
PMID:30976839

5. Brown DM, Parr T, Brameld JM. Myosin heavy chain mRNA isoforms are expressed in two distinct cohorts during C2C12 myogenesis. J Muscle Res Cell Motil. 2012; 32:383–90.
https://doi.org/10.1007/s10974-011-9267-4
PMID:22012579

6. Gard DL, Lazarides E. The synthesis and distribution of desmin and vimentin during myogenesis in vitro. Cell. 1980; 19:263–75.
https://doi.org/10.1016/0092-8674(80)90408-0
PMID:7188890

7. Liu QC, Zha XH, Faralli H, Yin H, Louis-Jeune C, Perdiguero E, Pranckeviciene E, Muñoz-Cànoves P, Rudnicki MA, Brand M, Perez-Iratxeta C, Dilworth FJ. Comparative expression profiling identifies differential roles for Myogenin and p38α MAPK signaling in myogenesis. J Mol Cell Biol. 2012; 4:386–97.
https://doi.org/10.1093/jmcb/mjs045
PMID:22847234

8. Hernández-Hernández JM, García-González EG, Brun CE, Rudnicki MA. The myogenic regulatory factors, determinants of muscle development, cell identity and regeneration. Semin Cell Dev Biol. 2017; 72:10–8.
https://doi.org/10.1016/j.semcdb.2017.11.010
PMID:29127045

9. Asfour HA, Allouh MZ, Said RS. Myogenic regulatory factors: The orchestrators of myogenesis after 30 years of discovery. Exp Biol Med (Maywood). 2018; 243:118–28.
https://doi.org/10.1177/1535370217749494
PMID:29307280

10. Sincennes MC, Brun CE, Lin AYT, Rosembert T, Datzkiw D, Saber J, Ming H, Kawabe YI, Rudnicki MA. Acetylation of PAX7 controls muscle stem cell self-renewal and differentiation potential in mice. Nat Commun. 2021; 12:3253.
https://doi.org/10.1038/s41467-021-23577-z
PMID:34059674

11. Seale P, Sabourin LA, Girgis-Gabardo A, Mansouri A, Gruss P, Rudnicki MA. Pax7 is required for the specification of myogenic satellite cells. Cell. 2000; 102:777–86.
https://doi.org/10.1016/s0092-8674(00)00066-0
PMID:11030621

12. O'Rourke JR, Georges SA, Seay HR, Tapscott SJ, McManus MT, Goldhamer DJ, Swanson MS, Harfe BD. Essential role for Dicer during skeletal muscle development. Dev Biol. 2007; 311:359–68.
https://doi.org/10.1016/j.ydbio.2007.08.032
PMID:17936265

13. Liu Y, Wang J, Zhou X, Cao H, Zhang X, Huang K, Li X, Yang G, Shi X. miR-324-5p Inhibits C2C12 cell Differentiation and Promotes Intramuscular Lipid Deposition through lncDUM and PM20D1. Mol Ther Nucleic Acids. 2020; 22:722–32.
https://doi.org/10.1016/j.omtn.2020.09.037
PMID:33230469

14. Wang H, Zhang Q, Wang B, Wu W, Wei J, Li P, Huang R. miR-22 regulates C2C12 myoblast proliferation and differentiation by targeting TGFBR1. Eur J Cell Biol. 2018; 97:257–68.
https://doi.org/10.1016/j.ejcb.2018.03.006
PMID:29588073

15. Kong D, He M, Yang L, Zhou R, Yan YQ, Liang Y, Teng CB. MiR-17 and miR-19 cooperatively promote skeletal muscle cell differentiation. Cell Mol Life Sci. 2019; 76:5041–54.
https://doi.org/10.1007/s00018-019-03165-7
PMID:31214725

16. Silva WJ, Graça FA, Cruz A, Silvestre JG, Labeit S, Miyabara EH, Yan CYI, Wang DZ, Moriscot AS. miR-29c improves skeletal muscle mass and function throughout myocyte proliferation and differentiation and by repressing atrophy-related genes. Acta Physiol (Oxf). 2019; 226:e13278.
https://doi.org/10.1111/apha.13278
PMID:30943315

17. Andersson U, Yang H, Harris H. High-mobility group box 1 protein (HMGB1) operates as an alarmin outside as well as inside cells. Semin Immunol. 2018; 38:40–8.
https://doi.org/10.1016/j.smim.2018.02.011
PMID:29530410

18. Careccia G, Saclier M, Tirone M, Ruggieri E, Principi E, Raffaghello L, Torchio S, Recchia D, Canepari M, Gorzanelli A, Ferrara M, Castellani P, Rubartelli A,

et al. Rebalancing expression of HMGB1 redox isoforms to counteract muscular dystrophy. Sci Transl Med. 2021; 13:eaay8416.
https://doi.org/10.1126/scitranslmed.aay8416
PMID:34078746

19. Kamiya M, Mizoguchi F, Kawahata K, Wang D, Nishibori M, Day J, Louis C, Wicks IP, Kohsaka H, Yasuda S. Targeting necroptosis in muscle fibers ameliorates inflammatory myopathies. Nat Commun. 2022; 13:166.
https://doi.org/10.1038/s41467-021-27875-4
PMID:35013338

20. Yang X, Xue P, Liu X, Xu X, Chen Z. HMGB1/autophagy pathway mediates the atrophic effect of TGF-β1 in denervated skeletal muscle. Cell Commun Signal. 2018; 16:97.
https://doi.org/10.1186/s12964-018-0310-6
PMID:30526602

21. Zong M, Bruton JD, Grundtman C, Yang H, Li JH, Alexanderson H, Palmblad K, Andersson U, Harris HE, Lundberg IE, Westerblad H. TLR4 as receptor for HMGB1 induced muscle dysfunction in myositis. Ann Rheum Dis. 2013; 72:1390–9.
https://doi.org/10.1136/annrheumdis-2012-202207
PMID:23148306

22. Brunn A, Zornbach K, Hans VH, Haupt WF, Deckert M. Toll-like receptors promote inflammation in idiopathic inflammatory myopathies. J Neuropathol Exp Neurol. 2012; 71:855–67.
https://doi.org/10.1097/NEN.0b013e31826bf7f3
PMID:22964787

23. Kim GT, Cho ML, Park YE, Yoo WH, Kim JH, Oh HJ, Kim DS, Baek SH, Lee SH, Lee JH, Kim HY, Kim SI. Expression of TLR2, TLR4, and TLR9 in dermatomyositis and polymyositis. Clin Rheumatol. 2010; 29:273–9.
https://doi.org/10.1007/s10067-009-1316-7
PMID:19953283

24. Muth IE, Zschüntzsch J, Kleinschnitz K, Wrede A, Gerhardt E, Balcarek P, Schreiber-Katz O, Zierz S, Dalakas MC, Voll RE, Schmidt J. HMGB1 and RAGE in skeletal muscle inflammation: Implications for protein accumulation in inclusion body myositis. Exp Neurol. 2015; 271:189–97.
https://doi.org/10.1016/j.expneurol.2015.05.023
PMID:26048613

25. Park JS, Svetkauskaite D, He Q, Kim JY, Strassheim D, Ishizaka A, Abraham E. Involvement of toll-like receptors 2 and 4 in cellular activation by high mobility group box 1 protein. J Biol Chem. 2004; 279:7370–7.
https://doi.org/10.1074/jbc.M306793200
PMID:14660645

26. Schmidt AM, Yan SD, Yan SF, Stern DM. The multiligand receptor RAGE as a progression factor amplifying immune and inflammatory responses. J Clin Invest. 2001; 108:949–55.
https://doi.org/10.1172/JCI14002
PMID:11581294

27. Lim MJ, Seo YH, Choi KJ, Cho CH, Kim BS, Kim YH, Lee J, Lee H, Jung CY, Ha J, Kang I, Kim SS. Suppression of c-Src activity stimulates muscle differentiation via p38 MAPK activation. Arch Biochem Biophys. 2007; 465:197–208.
https://doi.org/10.1016/j.abb.2007.06.004
PMID:17612500

28. Pegoraro V, Merico A, Angelini C. MyomiRNAs Dysregulation in ALS Rehabilitation. Brain Sci. 2019; 9:8.
https://doi.org/10.3390/brainsci9010008
PMID:30634563

29. Mahdy MAA. Glycerol-induced injury as a new model of muscle regeneration. Cell Tissue Res. 2018; 374:233–41.
https://doi.org/10.1007/s00441-018-2846-6
PMID:29754258

30. Mahdy MA, Lei HY, Wakamatsu J, Hosaka YZ, Nishimura T. Comparative study of muscle regeneration following cardiotoxin and glycerol injury. Ann Anat. 2015; 202:18–27.
https://doi.org/10.1016/j.aanat.2015.07.002
PMID:26340019

31. Kang X, Yang MY, Shi YX, Xie MM, Zhu M, Zheng XL, Zhang CK, Ge ZL, Bian XT, Lv JT, Wang YJ, Zhou BH, Tang KL. Interleukin-15 facilitates muscle regeneration through modulation of fibro/adipogenic progenitors. Cell Commun Signal. 2018; 16:42.
https://doi.org/10.1186/s12964-018-0251-0
PMID:30029643

32. Ho TL, Tang CH, Chang SL, Tsai CH, Chen HT, Su CM. HMGB1 Promotes In Vitro and In Vivo Skeletal Muscle Atrophy through an IL-18-Dependent Mechanism. Cells. 2022; 11:3936.
https://doi.org/10.3390/cells11233936
PMID:36497194

33. Chal J, Pourquié O. Making muscle: skeletal myogenesis *in vivo* and *in vitro*. Development. 2017; 144:2104–22.
https://doi.org/10.1242/dev.151035
PMID:28634270

34. Demonbreun AR, McNally EM. Muscle cell communication in development and repair. Curr Opin Pharmacol. 2017; 34:7–14.
https://doi.org/10.1016/j.coph.2017.03.008
PMID:28419894

35. Shi XC, Xia B, Zhang JF, Zhang RX, Zhang DY, Liu H, Xie BC, Wang YL, Wu JW. Optineurin promotes myogenesis during muscle regeneration in mice by autophagic degradation of GSK3β. PLoS Biol. 2022; 20:e3001619. https://doi.org/10.1371/journal.pbio.3001619 PMID:35476671

36. Biressi S, Filareto A, Rando TA. Stem cell therapy for muscular dystrophies. J Clin Invest. 2020; 130:5652–64. https://doi.org/10.1172/JCI142031 PMID:32946430

37. Day J, Otto S, Cash K, Eldi P, Hissaria P, Proudman S, Limaye V, Hayball JD. Aberrant Expression of High Mobility Group Box Protein 1 in the Idiopathic Inflammatory Myopathies. Front Cell Dev Biol. 2020; 8:226. https://doi.org/10.3389/fcell.2020.00226 PMID:32363191

38. Li L, Liu H, Tao W, Wen S, Fu X, Yu S. Pharmacological Inhibition of HMGB1 Prevents Muscle Wasting. Front Pharmacol. 2021; 12:731386. https://doi.org/10.3389/fphar.2021.731386 PMID:34867338

39. Chen R, Kang R, Tang D. The mechanism of HMGB1 secretion and release. Exp Mol Med. 2022; 54:91–102. https://doi.org/10.1038/s12276-022-00736-w PMID:35217834

40. Song J, Chowdhury IH, Choudhuri S, Ayadi AEI, Rios LE, Wolf SE, Wenke JC, Garg NJ. Acute muscle mass loss was alleviated with HMGB1 neutralizing antibody treatment in severe burned rats. Sci Rep. 2023; 13:10250. https://doi.org/10.1038/s41598-023-37476-4 PMID:37355693

41. Tirone M, Tran NL, Ceriotti C, Gorzanelli A, Canepari M, Bottinelli R, Raucci A, Di Maggio S, Santiago C, Mellado M, Saclier M, François S, Careccia G, et al. High mobility group box 1 orchestrates tissue regeneration via CXCR4. J Exp Med. 2018; 215:303–18. https://doi.org/10.1084/jem.20160217 PMID:29203538

42. Parrish W, Ulloa L. High-mobility group box-1 isoforms as potential therapeutic targets in sepsis. Methods Mol Biol. 2007; 361:145–62. https://doi.org/10.1385/1-59745-208-4:145 PMID:17172710

43. Lee G, Espirito Santo AI, Zwingenberger S, Cai L, Vogl T, Feldmann M, Horwood NJ, Chan JK, Nanchahal J. Fully reduced HMGB1 accelerates the regeneration of multiple tissues by transitioning stem cells to G_{Alert}. Proc Natl Acad Sci U S A. 2018; 115:E4463–72. https://doi.org/10.1073/pnas.1802893115 PMID:29674451

44. von Maltzahn J, Jones AE, Parks RJ, Rudnicki MA. Pax7 is critical for the normal function of satellite cells in adult skeletal muscle. Proc Natl Acad Sci U S A. 2013; 110:16474–9. https://doi.org/10.1073/pnas.1307680110 PMID:24065826

45. Lepper C, Partridge TA, Fan CM. An absolute requirement for Pax7-positive satellite cells in acute injury-induced skeletal muscle regeneration. Development. 2011; 138:3639–46. https://doi.org/10.1242/dev.067595 PMID:21828092

46. Padilla-Benavides T, Nasipak BT, Imbalzano AN. Brg1 Controls the Expression of Pax7 to Promote Viability and Proliferation of Mouse Primary Myoblasts. J Cell Physiol. 2015; 230:2990–7. https://doi.org/10.1002/jcp.25031 PMID:26036967

47. Oustanina S, Hause G, Braun T. Pax7 directs postnatal renewal and propagation of myogenic satellite cells but not their specification. EMBO J. 2004; 23:3430–9. https://doi.org/10.1038/sj.emboj.7600346 PMID:15282552

48. Kawai H, Nishino H, Kusaka K, Naruo T, Tamaki Y, Iwasa M. Experimental glycerol myopathy: a histological study. Acta Neuropathol. 1990; 80:192–7. https://doi.org/10.1007/BF00308923 PMID:2389683

49. Mahdy MAA, Warita K, Hosaka YZ. Glycerol induces early fibrosis in regenerating rat skeletal muscle. J Vet Med Sci. 2018; 80:1646–9. https://doi.org/10.1292/jvms.18-0328 PMID:30282842

50. Wang Y, Lu J, Liu Y. Skeletal Muscle Regeneration in Cardiotoxin-Induced Muscle Injury Models. Int J Mol Sci. 2022; 23:13380. https://doi.org/10.3390/ijms232113380 PMID:36362166

51. Ved R, Sharouf F, Harari B, Muzaffar M, Manivannan S, Ormonde C, Gray WP, Zaben M. Disulfide HMGB1 acts via TLR2/4 receptors to reduce the numbers of oligodendrocyte progenitor cells after traumatic injury in vitro. Sci Rep. 2021; 11:6181. https://doi.org/10.1038/s41598-021-84932-0 PMID:33731757

52. Paudel YN, Angelopoulou E, Piperi C, Othman I, Aamir K, Shaikh MF. Impact of HMGB1, RAGE, and TLR4 in Alzheimer's Disease (AD): From Risk Factors to Therapeutic Targeting. Cells. 2020; 9:383.

https://doi.org/10.3390/cells9020383
PMID:32046119

53. Chiappalupi S, Sorci G, Vukasinovic A, Salvadori L, Sagheddu R, Coletti D, Renga G, Romani L, Donato R, Riuzzi F. Targeting RAGE prevents muscle wasting and prolongs survival in cancer cachexia. J Cachexia Sarcopenia Muscle. 2020; 11:929–46. https://doi.org/10.1002/jcsm.12561 PMID:32159297

54. Ono Y, Maejima Y, Saito M, Sakamoto K, Horita S, Shimomura K, Inoue S, Kotani J. TAK-242, a specific inhibitor of Toll-like receptor 4 signalling, prevents endotoxemia-induced skeletal muscle wasting in mice. Sci Rep. 2020; 10:694. https://doi.org/10.1038/s41598-020-57714-3 PMID:31959927

55. Kim DS, Cha HN, Jo HJ, Song IH, Baek SH, Dan JM, Kim YW, Kim JY, Lee IK, Seo JS, Park SY. TLR2 deficiency attenuates skeletal muscle atrophy in mice. Biochem Biophys Res Commun. 2015; 459:534–40. https://doi.org/10.1016/j.bbrc.2015.02.144 PMID:25749338

56. Ge Y, Chen J. MicroRNAs in skeletal myogenesis. Cell Cycle. 2011; 10:441–8. https://doi.org/10.4161/cc.10.3.14710 PMID:21270519

57. Eisenberg I, Eran A, Nishino I, Moggio M, Lamperti C, Amato AA, Lidov HG, Kang PB, North KN, Mitrani-Rosenbaum S, Flanigan KM, Neely LA, Whitney D, et al. Distinctive patterns of microRNA expression in primary muscular disorders. Proc Natl Acad Sci U S A. 2007; 104:17016–21. https://doi.org/10.1073/pnas.0708115104 PMID:17942673

58. Tatsuguchi M, Seok HY, Callis TE, Thomson JM, Chen JF, Newman M, Rojas M, Hammond SM, Wang DZ. Expression of microRNAs is dynamically regulated during cardiomyocyte hypertrophy. J Mol Cell Cardiol. 2007; 42:1137–41. https://doi.org/10.1016/j.yjmcc.2007.04.004 PMID:17498736

59. Thum T, Galuppo P, Wolf C, Fiedler J, Kneitz S, van Laake LW, Doevendans PA, Mummery CL, Borlak J, Haverich A, Gross C, Engelhardt S, Ertl G, Bauersachs J. MicroRNAs in the human heart: a clue to fetal gene reprogramming in heart failure. Circulation. 2007; 116:258–67. https://doi.org/10.1161/CIRCULATIONAHA.107.687947 PMID:17606841

60. Chen JF, Tao Y, Li J, Deng Z, Yan Z, Xiao X, Wang DZ. microRNA-1 and microRNA-206 regulate skeletal muscle satellite cell proliferation and differentiation by repressing Pax7. J Cell Biol. 2010; 190:867–79. https://doi.org/10.1083/jcb.200911036 PMID:20819939

61. Yamaguchi T, Suzuki T, Arai H, Tanabe S, Atomi Y. Continuous mild heat stress induces differentiation of mammalian myoblasts, shifting fiber type from fast to slow. Am J Physiol Cell Physiol. 2010; 298:C140–8. https://doi.org/10.1152/ajpcell.00050.2009 PMID:19605738

62. Su CM, Tsai CH, Chen HT, Wu YS, Chang JW, Yang SF, Tang CH. Melatonin improves muscle injury and differentiation by increasing Pax7 expression. Int J Biol Sci. 2023; 19:1049–62. https://doi.org/10.7150/ijbs.79169 PMID:36923937

63. Wang YH, Tsai CH, Liu SC, Chen HT, Chang JW, Ko CY, Hsu CJ, Chang TK, Tang CH. miR-150-5p and XIST interaction controls monocyte adherence: Implications for osteoarthritis therapy. Front Immunol. 2022; 13:1004334. https://doi.org/10.3389/fimmu.2022.1004334 PMID:36203618

64. Rao X, Huang X, Zhou Z, Lin X. An improvement of the 2ˆ(-delta delta CT) method for quantitative real-time polymerase chain reaction data analysis. Biostat Bioinforma Biomath. 2013; 3:71–85. PMID:25558171

65. Achudhan D, Liu SC, Lin YY, Huang CC, Tsai CH, Ko CY, Chiang IP, Kuo YH, Tang CH. Antcin K Inhibits TNF-α, IL-1β and IL-8 Expression in Synovial Fibroblasts and Ameliorates Cartilage Degradation: Implications for the Treatment of Rheumatoid Arthritis. Front Immunol. 2021; 12:790925. https://doi.org/10.3389/fimmu.2021.790925 PMID:34975889

66. Wu MH, Lee TH, Lee HP, Li TM, Lee IT, Shieh PC, Tang CH. Kuei-Lu-Er-Xian-Jiao extract enhances BMP-2 production in osteoblasts. Biomedicine (Taipei). 2017; 7:2. https://doi.org/10.1051/bmdcn/2017070102 PMID:28474578

SUPPLEMENTARY MATERIALS

Supplementary Table

Supplementary Table 1. Primers sequences for qRT-PCR.

Genes	Forward (5′–3′)	Reverse (5′–3′)
Pax-7	GGTCCCCAGGATGATGAGA	TTGATGAAGACCCCACCAAG
GAPDH	ACCACAGTCCATGCCATCAC	TCCACCACCCTGTTGCTGTA
miR-185-3p	AGGGGCTGGCTTTCCTCTGGT	TGGTGTCGTGGAGTCG
miR-206-3p	TGGAATGTAAGGAAGTGTGTGG	TGGTGTCGTGGAGTCG
miR-342-5p	AGGGGTGCTATCTGTGATTGAG	TGGTGTCGTGGAGTCG
miR-499-3p	GAACATCACAGCAAGTCTGTGCT	TGGTGTCGTGGAGTCG
miR-742-3p	GAAAGCCACCATGCTGGGTAAA	TGGTGTCGTGGAGTCG
miR-1194	TCCTAGATCGTCAATGAGTAAG	TGGTGTCGTGGAGTCG
miR-133c	TTTGGTCCCCTTCAAGGAGTCAG	TGGTGTCGTGGAGTCG
miR-133b-3p	TTTGGTCCCCTTCAACCAGCTA	TGGTGTCGTGGAGTCG
miR-1949	CTATACCAGGATGTCAGCATAGTT	TGGTGTCGTGGAGTCG
miR-3078-3p	TTGCTGGGGTAGTCTTTAGG	TGGTGTCGTGGAGTCG
miR-3475-3p	TCTGGAGGCACATGGTTTGAA	TGGTGTCGTGGAGTCG
miR-5127	TCTCCCAACCCTTTTCCCA	TGGTGTCGTGGAGTCG
U6 snRNA	CTCGCTTCGGCAGCACA	AACGCTTCACGAATTTGCGT